






Type 2A and 2M von Willebrand Disease: Differences in Phenotypic Parameters According to the Affected Domain by Disease-Causing Variants and Assessment of Pathophysiological Mechanisms

Adriana Inés Woods, PhD¹ Juvenal Paiva, MS² Débora Marina Primrose, PhD³
Alicia Noemí Blanco, PhD² Analía Sánchez-Luceros, MD, PhD^{1,2}

¹Laboratorio de Hemostasia y Trombosis, IMEX-CONICET-Academia Nacional de Medicina de Buenos Aires. CABA, Argentina

²Departamento de Hemostasia y Trombosis, Instituto de Investigaciones Hematológicas, Academia Nacional de Medicina de Buenos Aires. CABA, Argentina

³Química de los Alimentos, Facultad de Agronomía y Ciencias Agroalimentarias, Universidad de Morón. Buenos Aires, Argentina

Address for correspondence: Adriana Inés Woods, PhD, Laboratorio de Hemostasia y Trombosis, IMEX-CONICET-Academia Nacional de Medicina de Buenos Aires. CABA, Argentina (e-mail: aiwoods@hematologia.anm.edu.ar; adrianawoods@gmail.com).

Semin Thromb Hemost 2021;47:862–874.

Abstract

Type 2A and 2M von Willebrand disease (VWD) broadly show similar phenotypic parameters, but involve different pathophysiological mechanisms. This report presents the clinical and laboratory profiles of type 2A and type 2M patients genotypically diagnosed at one large center. Higher bleeding score values and a higher incidence of major bleeding episodes were observed in type 2A compared with type 2M, potentially reflective of the absence of large and intermediate von Willebrand factor (VWF) multimers in 2A. In type 2A, most of disease-causing variants (DCVs) appeared to be responsible for increased VWF clearance and DCV clustered in the VWF-A1 domain resulted in more severe clinical profiles. In type 2M, DCV in the VWF-A1 domain showed different laboratory patterns, related to either reduced synthesis or shortened VWF survival, and DCV in the VWF-A2 domain showed patterns related mainly to shortened survival. VWF-type 1 collagen binding/Ag (C1B/Ag) showed different patterns according to DCV location: in type 2A VWD, C1B/Ag was much lower when DCVs were located in the VWF-A2 domain. In type 2M with DCV in the VWF-A1 domain, C1B/Ag was normal, but with DCV in the VWF-A2 domain, C1B/Ag was low. The higher frequency of major bleeding in VWD 2M patients with DCV in the VWF-A2 domain than that with DCV in the VWF-A1 domain could be a summative effect of abnormal C1B/Ag, on top of the reduced VWF-GPIb binding. In silico modeling suggests that DCV impairing the VWF-A2 domain somehow modulates collagen binding to the VWF-A3 domain. Concomitant normal FVIII:C/Ag and VWFpp/Ag, mainly in type 2M VWD, suggest that other nonidentified pathophysiological mechanisms, neither related to synthesis/retention nor survival of VWF, would be responsible for the presenting phenotype.

Keywords

- ▶ disease-causing variants
- ▶ phenotype–genotype
- ▶ von Willebrand disease
- ▶ von Willebrand factor
- ▶ collagen binding

von Willebrand disease (VWD) is the most common inherited bleeding disorder, and comprises quantitative (types 1 and 3) or qualitative (types 2A, 2B, 2M, and 2N) defects of von Willebrand factor (VWF).¹ Type 2M is probably as common as type 2A; however, it can be underreported due to misidentification.² In our population cohort, type 2M was found to be more frequent than type 2A.³ Laboratory parameters are broadly similar in types 2A and 2M; they both show reduced levels of VWF activity compared with VWF:Ag (Ag) and also reduced ristocetin-induced platelet aggregation (RIPA). However, there are subtle differences in phenotypic patterns. For example, low VWF collagen binding (VWF:CB) compared with Ag is generally evident in type 2A VWD, but only in some cases of type 2M. A generally accepted consensus is to define type 2A and type 2M using a cut-off value below 0.6 for VWF activity/protein ratio^{4–8}; that is VWF:RCo/VWF:Ag (-RCo/Ag),⁷ VWF:GPIbM/Ag, VWF:GPIbR/Ag, and/or low VWF:CB/Ag (CB/Ag).⁸ Differential phenotypic diagnosis can be assisted by performing multimeric analysis.^{5,9}

Type 2A VWD is characterized by the absence of high-molecular-weight VWF multimers (HMWMs) in both plasma and platelets and, in some cases, the absence also of intermediate-molecular-weight multimers (IMWMs),¹ and also by generally observed low CB/Ag. Responsible disease-causing variants (DCVs) in the VWF gene are mainly missense, mostly clustered in the VWF-A2 domain.¹⁰ In type 2M VWD, characterized by the presence of a normal multimeric profile,¹ the dysfunctional proteins arising generally lead to defects in VWF binding to platelets, thus showing low GPIb binding activity/Ag (i.e., low RCo/Ag, VWF:GPIbR/Ag, and/or VWF:GPIbM/Ag)⁵ but usually normal CB/Ag,^{11,12} although abnormal CB/Ag values have also been reported in some cases.¹³ Type 2M VWD is usually caused by dominant DCVs mostly clustered in the VWF-A1 domain.^{7,10} These DCVs can either affect VWF-GPIb binding or enhance the stability of the VWF-A1 domain, thereby reducing the rate of unfolding VWF-A1 domain under flow.¹⁴ Additionally, DCVs in the VWF-A3 domain have also been described (VWF:CB binding defects); these reduce VWF-collagen binding, also causing type 2M VWD, but generally with normal RCo/Ag.^{15,16}

Both factor VIII coagulant activity/Ag (FVIII:C/Ag) and VWF propeptide/Ag (VWFpp/Ag) have been associated with different pathophysiological mechanisms related to DCVs in type 1 VWD.¹⁷ Moreover, they have also been considered a useful tool in the diagnosis of type 2 and 3 VWD.¹⁸ FVIII:C/Ag increases when VWF synthesis is reduced, but is near unity when the half-life of VWF is decreased.¹⁹ In contrast, VWFpp/Ag does not change when the synthesis is reduced, but increases when VWF is cleared faster.¹⁷ It has been reported that patients with DCVs showing complete co-segregation between phenotype and genotype have higher FVIII:C/Ag and VWFpp/Ag values than in those with incomplete co-segregation.¹⁷

The aim of this study is to describe the differences observed between clinical and laboratory phenotypes in patients with type 2A and 2M VWD, depending on the affected domains (DCVs located in exon 28 of the VWF gene, but sometimes also exons 29–31) and the possible pathophysiological mechanisms involved.

Materials and Methods

Subjects

A total of 106 affected family members (AFMs) belonging to 31 unrelated families (32 index cases) were recruited and phenotypically and genotypically characterized. AFMs were diagnosed at different life stages: childhood (type 2A: 26.6%, type 2M: 39.2%), adolescence (type 2A: 16.6%, type 2M: 10.8%), adults before (type 2A: 33.4%, type 2M: 35.1%) or after age 50 (type 2A: 23.4%, type 2M: 14.9%). Furthermore, 31 unaffected relatives were also evaluated, to estimate the penetrance of the disease within families and the prevalence of causative DCVs. All subjects were Caucasian and no cases of consanguinity were reported in any of the families. All the participants involved in the study were evaluated after giving their written informed consent; the information collected remained anonymous and confidential. This study was approved by the local ethics committee.

One-hundred healthy random controls were assessed to estimate the frequency in our geographic region of possible polymorphic variants of the VWF gene and to estimate the possible implication of the novel DCVs in phenotypes.

Inclusion Criteria

All subjects met the criteria for diagnosis of type 2A or 2M VWD: personal and/or family bleeding history and laboratory profile including RCo/Ag < 0.6, low or absent RIPA at normal ristocetin challenge dose (1.2 mg/mL), and either lack of HMWM and potentially also IMWM for type 2A or presence of IMWM and HMWM for type 2M.

Clinical Profile

Each patient's bleeding phenotype was appraised by analyzing individual anamnestic data collected by hematologists during the initial consultation. Symptoms were scored applying the International Society on Thrombosis and Haemostasis/Scientific and Standardization Committee bleeding assessment tool (ISTH-BAT) considering normal bleeding score: 0–3 in adult males,²⁰ 0–5 in adult females, and 0–2 in children, both male and female.²¹ The pictorial bleeding assessment chart (PBAC) was applied to categorize menstrual bleeding, with menorrhagia being considered when the score was ≥ 185 .²² Major bleeding was defined as: fatal bleeding; intracranial, intraspinal, retroperitoneal/peritoneal, pericardial, or intraocular bleeding; bleedings that required blood transfusion of more than 2 units of whole blood or red cells, or which caused a hemoglobin drop greater than 20 g/dL²³ or requiring either administration of VWF concentrates, blood derivative transfusion, desmopressin (DDAVP), hospitalization, or surgical intervention.

Laboratory Assays

The following tests were performed, the method and reference range for each test are shown in parentheses: FVIII:C (one-stage method; 50–150 IU/dL)²⁴; VWF:Ag (enzyme-linked-immunosorbent assay [ELISA]; 50–150 IU/dL)²⁵; VWF:RCo (aggregometry, fixed-washed platelets; 50–150

IU/dL)²⁶; type I collagen binding activity (VWF:C1B) (ELISA; 60–130 IU/dL) (Technozym # cat 5450311, Technoclone GmbH, Vienna Austria); VWFpp (ELISA; 50–150 IU/dL).²⁷ The ratios FVIII:C/Ag (0.8–1.4), RCo/Ag (cut off value > 0.6), C1B/Ag (cut off value > 0.6), and VWFpp/Ag (0.92–2.14) were calculated for each patient. VWF multimeric analysis was performed by 1% sodium dodecyl sulphate and 1.7% agarose gel electrophoresis, as previously described.²⁸ RIPA was performed at 1.2, 1.5, and 2.0 mg/mL ristocetin, and also 0.7 mg/mL to exclude 2B VWD. A local normal plasma pool, obtained from 20 healthy donors, was used as a secondary standard, calibrated against the standard 07/316 from the National Institute for Biological Standards and Control.

Genotypic Analysis

Genomic DNA was extracted from peripheral blood leucocytes. Exon 28 of the *VWF* gene was amplified by a polymerase chain reaction as previously described²⁹ and sequenced by automated Sanger sequencing technology. When a causative variant was identified, the opposite DNA strand was sequenced to confirm the presence of the sequence variations. Exons 29 to 31 were also amplified in those patients with a DCV identified in the VWF-A2 domain, to check the VWF-A3 domain.

In Silico Bioinformatics Analysis and Sequence Alignment

The in silico analysis of novel missense changes was performed using the following informatics applications: PolyPhen-2 (<http://genetics.bwh.harvard.edu/pph2/>), Mutation Taster (<http://www.mutationtaster.org/>), SIFT (<http://sift.bii.a-star.edu.sg/>), and Provean (<http://provean.jcvi.org/index.php>). I-mutant suite was used to predict effects of single-point protein variant on its stability by measuring the change in the Gibbs free energy upon folding (DDG) (<http://gpcr2.biocomp.unibo.it/cgi/predictors/I-Mutant3.0/I-Mutant3.0.cgi>). DDG values within -0.5 to 0.5 kcal/mol mean neutral stability; values >0.5 kcal/mol suggest a large increase of stability, and values <-0.5 kcal/mol suggest a large decrease of stability. The sequence alignment of the protein was performed using UniProtKB and compared with the reference sequence (NM_000552.5) (www.uniprot.org). Varsome (<https://varsome.com>) and Genome Aggregation Database (GnomAD) were accessed to check the registry (if any) of novel variants and their minor allele frequency (MAF) (<https://gnomad.broadinstitute.org/>).

In Silico Modeling Analysis

To determine differences in the VWF-type I collagen binding of patients with DCV in the VWF-A2 domain, models for the mutant VWF were constructed. Using Swiss-PDBviewer, the leucine of the crystal structure of the VWF-A2 domain (3ZQK.A) was substituted by proline to make the missense mutation p.L1503P (<http://www.expasy.org/spdbv/>).³⁰ Similarly, the mutated VWF-A2 domains p.G1505R, p.Y1542D, p.E1549K, p.R1564W, p.R1597W, p.I1628T, p.G1631D, and p.F1654L were likewise produced by substitution of the mutated residue.

The hypothetical complex structure of the three domains of VWF was obtained using the protein–protein docking server ClusPro2.0 (<http://cluspro.bu.edu>).³¹ The crystal structure 1SQ0.A was used for the VWF-A1 domain and 1A03.A was used for the VWF-A3 domain. The crystal structure 3ZQK.A was used for the VWF-A2 domain in the wild-type (WT) model and the mutated VWF-A2 domains generated by Swiss-PDBviewer were used respectively for each mutated VWF. To gain graphical comprehension of the interaction between type I collagen and all three VWF domains, in silico docking simulations were performed using the PatchDock server (<http://bioinfo3d.cs.tau.ac.il/Patch-Dock>).³² For this, the X-ray diffraction-solved crystal structure of the VWF binding to type I collagen (3HQV) was docked with the VWF models previously obtained. All models were tested using Procheck in PDBsum (<http://www.ebi.ac.uk>),³³ having at least 99.2% of the residues in the most favored regions and in the additionally allowed regions. Molecular graphics were performed with the UCSF Chimera package (<http://www.cgl.ucsf.edu/chimera>).³⁴ The H-bonds were obtained using structure analysis in UCSF Chimera with a tolerance of 0.4 \AA and 20.0 degrees. To compare models, root mean square deviation (RMSD) between all corresponding α carbon in the α and β chains was calculated using Swiss-PDBviewer after iterative magic fit. RMSD was used to evaluate the differences in docking orientation of the three VWF domains and of the collagen binding with the VWF-A3 domain of each DCV model compared with the WT VWF model. We used three different RMSD classifications for protein superposition: same binding orientation when RMSD was less than 2.0 \AA ; very similar when RMSD was between 2.0 and 3.0 \AA ; and different binding orientation when RMSD was greater than 3.0 \AA . Accessibility was assessed using the same program to show residues with at least 30% surface contact (<http://www.expasy.org/spdbv/>).³⁰ As a control, the hypothetical model of the VWF with one of the most common DCV in the VWF-A1 domain p.R1374C was docked with collagen.

Assignment of Genetic Variants as “Disease-Causing Variant”

We follow the recommendations of the Human Genome Variation Society (HGVS) (<http://www.hgvs.org>), the American College of Medical Genetics (<http://www.acmg.net>), and the HGVS nomenclature (<https://varnomen.hgvs.org/>), which suggest to consider the use of “disease-causing variant” to describe “pathogenic” and/or “likely pathogenic,” variants identified in genes that cause Mendelian disorders. This term “disease-causing variant” was also adopted for many other research groups and it is also used in the ACGS Best Practice Guidelines for Variant Classification in Rare Disease 2020 (<https://www.bsgm.org.uk/>). The genotypic variants that were found in our patients were considered “disease causing” given the concomitant finding of clinical and laboratory parameters in patients (personal bleeding history and abnormal laboratory profiles), and the in silico predictions and modeling results.

Statistical Analysis

Descriptive statistical analysis was performed considering mean values (\bar{x}) and standard deviation) for continuous variables. Median values were used for those data with distribution bias (bleeding score and age). Comparative analysis was performed using chi-square test with Yates's correction or Student's *t*-test, as appropriate. The Kruskal–Wallis test was applied to compare frequencies. *p*-Values <0.05 were considered statistically significant. Difference between proportions and Spearman's rank correlation coefficient (Spearman's rho) were also calculated. Relative risk (RR) with 95% confidence interval (CI) was used to show the strength of the association within different phenotypic parameters. The prevalence of DCV³⁵ and the penetrance of VWD within families with ≥ 2 generations were calculated.

Results

Clinical Phenotype Profile of Patients

Thirty-one patients (29.5%) were diagnosed as type 2A VWD (belonging to 12 families) and 75 (70.5%) as type 2M VWD (belonging to 21 families). Among the AFMs, 65.3% had O blood group and 55.3% were females; the median of age was 21 years (range: 1–82). All the unaffected relatives available for analysis displayed both normal clinical and laboratory phenotype, and they did not carry any DCV in exon 28.

Major bleeding was observed in 48.4% of type 2A patients and in 38.7% of type 2M patients. Among type 2A patients, 31 episodes of major bleeding were documented (average 1 episode/patient), while 42 episodes were reported in type 2M patients (average: 0.57 episodes/patient) with statistically significant difference ($p < 0.0001$). The descriptions of frequency of bleeding symptoms and their association with episodes of major bleeding are shown in **Table 1**.

Bleeding score was higher in type 2A patients (7.3 ± 3.6) than in type 2M patients (4.8 ± 3) ($p = 0.0004$). A strong direct relationship was observed between bleeding score and major bleeding with RR = 2.34 (95% CI: 1.25–4.41) for type 2A patients and RR = 3.77 (95% CI: 2.25–6.31) for type 2M patients.

To analyze the variability of the bleeding score within each family and among families with the same DCV, we selected families with ≥ 2 AFM studied: six families with type 2A and 10 families with type 2M VWD. A wide variability in bleeding score was observed not only in AFM within the same family, but also among different families carrying the same DCV (**Table 2**).

Genotypic analysis

In type 2A patients, seven DCVs were identified in exon 28: one in the VWF-A1 domain and six in the VWF-A2 domain, with p.R1597W (VWF-A2 domain) the most frequent DCV (16 AFMs in four families).

In type 2M patients, 14 DCVs were identified in exon 28: nine located in the VWF-A1 domain and four in the VWF-A2 domain. The most frequent DCV was p.E1549K (VWF-A2 domain), detected in 32 AFMs from a four-generation family and in one unrelated patient.

DCVs were found in the heterozygous state in all the AFMs; only two type 2M patients (two sisters) were homozygous for p.R1374C.

Exons 29, 30, and 31 encoding for the VWF-A3 domain was found normal in both type 2A and type 2M patients with DCV located in the VWF-A2 domain.

Three variants were detected in a 17-year-old female (not included in **Table 3**) showing a 2A phenotype. She presented severe epistaxis, menorrhagia (PBAC > 1,000) and severe anemia (bleeding score = 10), FVIII:C = 45 IU/dL, VWF:Ag = 39 IU/dL, FVIII:C/Ag = 1.15, VWF:RCo < 5 IU/dL, RCo/Ag = 0.13, VWF:C1B = 7 IU/dL, C1B/Ag = 0.23, and VWFpp/Ag = 1.85. Multimeric profile: absence of HMWM and IMWM. The three variants were: p.P1266Q, which has been described as a type 2M VWD,³⁶ as a VWF gene conversion variant resulting in type 2M VWD,³⁷ and also as a type 2B VWD³⁸; p.L1603P previously described as related to type 1 VWD (<http://www.ragtimedesign.com/vwf/mutation/>) and also as type 2A VWD³⁹; and a novel c.4136G > A → p.R1379H. This last change of arginine for histidine at position R1379 was predicted as possibly damaging by the Poly-Phen-2 and SIFT, disease causing by Mutation Taster, and neutral

Table 1 Frequency of bleeding symptoms and their association with episodes of major bleeding

Bleeding symptom	Type 2A patients		Type 2M patients	
	Frequency	With major bleeding	Frequency	With major bleeding
Epistaxis	58.1% (18/31)	27.8% (5/18)	57.3% (43/75)	11.6% (5/43)
Menorrhagia	80% (12/15)	25% (3/12)	75.7% (28/37)	21.4% (6/28)
Tooth extraction	46.6% (7/15)	0% (0/7)	64.7% (22/34)	13.6% (3/22)
Surgeries	66.7% (8/12)	50% (4/8)	51.9% (14/27)	57.1% (8/14)
Vaginal delivery	66.7% (8/12)	62.5% (5/8)	33.4% (4/12)	50% (2/4)
Cesarean section	100% (1/1)	100% (1/1)	50% (3/6)	66.7% (2/3)
Easy bruising	70.9% (22/31)	0% (0/22)	52% (39/75)	5.1% (2/39)
Gum bleeding	38.7% (12/31)	8.3% (1/12)	24% (18/75)	100% (0/18)
Gastrointestinal bleeding	12.9% (4/31)	100% (4/4)	8% (7/75)	100% (7/7)

Table 2 Variability of the bleeding score within affected family members and families

Affected family members in each family (family/n)	Bleeding score median (range)	Disease-causing variant
Type 2A patients		
F1/2	9 (8–10)	p.C1272F
F2/3	4 (4–10)	p.G1505R
F3/5	3.5 (3–8)	p.R1597W
F4/8	4 (1–10)	p.R1597W
F5/3	8 (2–10)	p.I1628T
F6/2	8 (5–11)	p.I1628T
Type 2M patients		
F7/2	5 (4–6)	p.F1293C
F8/2	5 (3–7)	p.R1374C
F9/3	7 (4–7)	p.R1374C
F10/6	1.5 (0–4)	p.R1374C
F11/4	3 (2–5)	p.R1374C
F12/6	4.5 (2–7)	p.R1374C
F13/4	9 (5–13)	p.A1437T
F14/2	7.5 (4–13)	p.L1503P
F15/32	5 (0–12)	p.E1549K
F16/4	2 (1–8)	p.I1628T

by Provean. I-Mutant predicted a large decrease of VWF stability (−1.28 kcal/mol). Varsome showed an allelic frequency of 0.00003434, with no publications found regarding this variant. In the GnomAD, this variant has been described as missense, with its MAF of 1.78×10^{-5} (5/281,388 alleles). Multiple sequence alignment showed that the residue R1379 is located in a highly conserved area of the VWF gene, suggesting a damaging effect of the change from arginine to histidine on the mutant protein.

This novel variant was not associated with a defined phenotype. It was not found in any of the 100 healthy controls (200 alleles) analyzed in this study; therefore, it was not considered as single-nucleotide variant in our general population. The combination of these three variants (p.P1266Q, p.L1603P, and p.R1379H), in our patient, thus resulted in her type 2A phenotype.

The prevalence of DCVs in our patients' families was estimated to be 0.84% (95% CI: 0.75–0.9); the same DCV was present in all generations available in each family. So, the penetrance of VWD was complete.

Clinical and Laboratory Profiles According to the Affected Domain by DCVs

To compare clinical and laboratory profiles depending on affected domains, both type 2A and 2M patients were grouped according the location of DCVs (►Table 3). Differences were found between type 2A and 2M patients with

DCVs affecting the same domain; furthermore, those profiles were also different between VWF-A1 and VWF-A2 domains within the same VWD type.

DCV in the VWF-A1 Domain

When DCVs were located in the VWF-A1 domain, type 2A showed both higher percentage of patients with major bleeding and frequency of episodes/patient, and a slightly higher bleeding score when compared with type 2A patients with DCV in the VWF-A2 domain, showing a very weak positive correlation with major bleeding ($\rho = 0.15$; RR = 2.23; 95% CI: 1.49–3.34). However, given the very small number of AFM ($n = 2$), the difference between proportions was not significant. Type 2A versus type 2M showed that type 2A also had higher percentage of patients with major bleeding, frequency of episodes/patient (1 episode/patient), and bleeding score, although only the bleeding score was statistically significant ($p = 0.015$).

Type 2M patients with DCV in the VWF-A1 domain had lower VWF:Ag ($p = 0.0001$) and VWFpp ($p = 0.007$), but higher FVIII:C/Ag ($p < 0.0001$) and VWFpp/Ag ($p = 0.018$) than type 2M patients with DCV in the VWF-A2 domain.

DCV in the VWF-A2 Domain

Type 2A versus type 2M showed that type 2A patients had a higher bleeding score ($p = 0.02$), a lower VWF:Ag ($p = 0.001$), and a higher VWFpp/Ag ($p = 0.005$).

Type 2M with DCV in the VWF-A2 domain showed a higher percentage of patients with major bleeding and frequency of episodes/patient compared with those of type 2M with DCV in the VWF-A1 domain ($p = 0.004$).

C1B/Ag According to the Affected Domains

The analysis of C1B/Ag according to location of DCV showed differences in results: in type 2A patients, C1B/Ag was low in all cases, but lower when DCVs were located in the VWF-A2 domain ($p = 0.028$). Type 2M patients with DCV in the VWF-A1 domain showed normal C1B/Ag, whereas those with DCV in the VWF-A2 domain showed low C1B/Ag (below the cut-off value) ($p = 0.0001$).

FVIII:C/Ag and VWFpp/Ag Analysis

To analyze the different pathophysiological mechanisms involved in type 2A and 2M VWD, FVIII:C/Ag and VWFpp/Ag ratios were analyzed according to DCVs and their location in the VWF-A1 and VWF-A2 domains. In both type 2A and type 2M, values of FVIII:C/Ag and VWFpp/Ag yielded different results according to DCV, as shown in ►Table 4.

A comparison of FVIII:C/Ag and VWFpp/Ag ratios between locations of DCVs in the VWF-A1 and VWF-A2 domains is shown in ►Table 5.

In Silico Modeling Analysis

A hypothetical in silico model of VWF was obtained by protein interactions between VWF-A1, VWF-A2, and VWF-A3 domains. In this model, the VWF-A2 domain is flanked by VWF-A1 and VWF-A3 domains. The VWF-A2 domain is formed by six β -sheets making a hydrophobic central core

Table 3 Comparison of clinical and laboratory profiles of type 2A and type 2M VWD patients according to the affected domain

Type 2A			
Domain	A1	A2	p-Values
Patients, <i>n</i>	2	29	
Patients with major bleeding	100%	44.8%	0.226
Episodes/patient	2.5	0.9	
Bleeding score, median (range)	10.5 (10–11)	6 (2–15)	0.175
FVIII:C, IU/dL	32.5 ± 3.5	45.8 ± 18.5	0.325
VWF:Ag, IU/dL	38 ± 8.5	43.2 ± 21.2	0.736
FVIII:C/Ag	0.9 ± 0.1	1.3 ± 0.7	0.433
Patients with >1.4	0%	27.6%	
VWF:RCo, IU/dL	1.0 ± 0.0	4.4 ± 3.1	0.137
RCo/Ag	0.24 ± 0.03	0.2 ± 0.25	0.825
VWF:C1B, IU/dL	17 ± 0.1	10 ± 5.8	0.103
C1B/Ag	0.46 ± 0.1	0.2 ± 0.1	0.028
VWFpp, IU/dL	100.5 ± 41.8	110.5 ± 38.8	0.725
VWFpp/Ag	3.3 ± 0.2	2.7 ± 1.1	0.454
Patients with >2.14	100%	76.9%	
Type 2M			
Patients, <i>n</i>	36	39	
Patients with major bleeding	29.4%	48.7%	0.149
Episodes/patient	0.38	0.74	0.004
Bleeding score, median (range)	4 (0–20)	5 (0–14)	0.394
FVIII:C, IU/dL	57.5 ± 27.4	54.6 ± 20.5	0.605
VWF:Ag, IU/dL	33.4 ± 23.6	61.8 ± 21.2	0.0001
FVIII:C/Ag	2.1 ± 1.1	1.0 ± 0.4	0.0001
Patients with >1.4	67.6%	10%	0.0001
VWF:RCo, IU/dL	7.2 ± 8.3	5.4 ± 4.8	0.253
RCo/Ag	0.2 ± 0.2	0.2 ± 0.1	1.000
VWF:C1B, IU/dL	34.8 ± 10.5	9.2 ± 0.6	0.0001
C1B/Ag	0.9 ± 0.2	0.2 ± 0.1	0.0001
VWFpp, IU/dL	72.7 ± 30.6	112.5 ± 53.7	0.007
VWFpp/Ag	2.5 ± 0.9	1.9 ± 0.7	0.018
Patients with >2.14	62.5%	40.9%	0.091

Abbreviations: FVIII:C, factor VIII coagulant activity; VWD, von Willebrand disease; VWF:Ag, von Willebrand factor antigen; FVIII:C/Ag, FVIII:C/VWF:Ag; VWF:RCo, ristocetin cofactor activity; RCo/Ag, VWF:RCo/VWF:Ag; VWF:C1B, type I collagen-binding activity; C1B/Ag, VWF:C1B/VWF:Ag; VWFpp, VWF propeptide; VWFpp/Ag, VWF propeptide/VWF:Ag.

Note: The values are expressed as mean ± 2 standard deviation and in some cases as median/range. Bold font *p*-values are those showing statistical significance.

surrounded by five α -helices. The β -sheets are joined to the α helices by flexible loops, except for the exceptionally long loop between β 3- and β 4-sheets, with no α -helix between these sheets. The ADAMTS-13 (a disintegrin and metalloproteinase with a thrombospondin type 1 motif, member 13) cleavage site at Y1605 and M1606 is in the middle of the β 4-sheet, deeply buried in the VWF-A2 hydrophobic core. ► **Fig. 1** shows some of in silico modeling of DCVs.

Modeling of DCV p.R1379H

The R1379 forms a strong H-bond with I1410 (2.82 Å), L1407 (2.57 Å), and L1371 (2.41 Å), while the mutant H1379 only keeps I1410 (2.82 Å), losing the rest of the H-bonds, resulting in a large decrease of VWF stability (–1.28 kcal/mol). The model of this variant located in the VWF-A1 domain docked with collagen showed no differences (RMSD of 0.00 Å) with the WT-VWF model, also docked with type I collagen.

Table 4 FVIII:C/Ag and VWFpp/Ag ratios in type 2A and 2M VWDs according to the DCV

DCV	Only high FVIII:C/Ag	Only high VWFpp/Ag	Both high ratios	Both normal ratios	Pathophysiological mechanism involved in each DCV
Type 2A VWD					
p.C1272F		100% of cases			Reduced survival
p.G1505R		66.7% of cases	33.3% of cases		Mainly reduced survival; in some cases, both mechanisms
p.Y1542D	100% of cases				Reduced synthesis/intracellular retention
p.R1597W		66.7% of cases	33.3% of cases		Mainly reduced survival; in some cases, both mechanisms
p.I1628T		33.3% of cases	33.3% of cases	33.3% of cases	Reduced survival; in some cases, both mechanisms and other not known mechanism
p.G1631D		100% of cases			Reduced survival
p.F1654L				100% of cases	Other not known mechanism
Type 2M VWD					
p.P1266Q				100% of cases	Other not known mechanism
p.F1293C			100% of cases		Both mechanisms
p.G1324S				100% of cases	Other not known mechanism
p.S1325F				100% of cases	Other not known mechanism
p.R1334Q				100% of cases	Other not known mechanism
p.R1374C	12.5% of cases	6.25% of cases	75% of cases	6.25% of cases	Mainly both mechanisms
p.R1374L				100% of cases	Other not known mechanism
p.K1408del	100% of cases				Reduced synthesis/intracellular retention
p.A1437T	50% of cases	50% of cases			Reduced synthesis/intracellular retention; reduced survival
p.T1468I				100% of cases	Other not known mechanism
p.L1503P	50% of cases			50% of cases	Other not known mechanism
p.E1549K		43.7% of cases		56.3% of cases	Mainly other not known mechanism; in some cases, reduced survival
p.R1564W	100% of cases				Reduced synthesis/intracellular retention
p.I1628T			33.3% of cases	66.7% of cases	Mainly other not known mechanism

Abbreviations: DCV, disease-causing variant; FVIII:C/Ag, FVIII:C/VWF:Ag; VWD, von Willebrand disease; VWFpp/Ag, VWF propeptide/VWF:Ag.

Table 5 VIII:C/Ag and VWFpp/Ag ratios according to the affected domain by DCV

VWD variant	Type 2A		Type 2M	
	A1 (n: 2)	A2 (n: 13)	A1 (n: 27)	A2 (n: 21)
Percentage of patients with				
High FVIII:C/Ag	0	30.8	66.6	19.0
High VWFpp/Ag	100	76.9	59.3	38.1
Only high FVIII:C/Ag	0	7.7	14.8	9.5
Only high VWFpp/Ag	100	53.8	7.4	33.3
Both ratios high	0	23.1	51.9	4.8
Both ratios normal	0	15.4	25.9	52.4

Abbreviations: DCV, disease-causing variant; FVIII:C/Ag, FVIII:C/VWF:Ag; VWFpp/Ag, VWF propeptide/VWF:Ag.

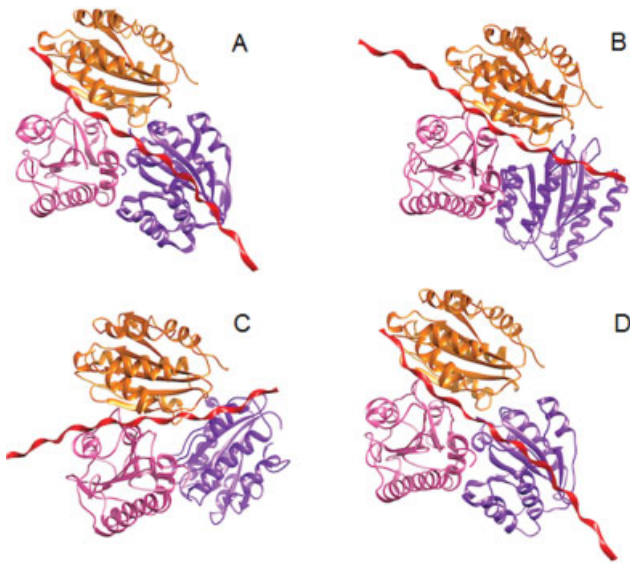


Fig. 1 Hypothetical model of collagen (3HQV) with von Willebrand factor (VWF). Type I collagen (red) with VWF-A1 (orange), VWF-A2 (pink), and VWF-A3 (purple) domains of VWF are shown: (A) A2 wild-type VWF; (B) mutated VWF-A2p.L1503P; (C) mutated VWF-A2 p.E1549K; (D) control (mutated VWF-A1 p.R1374C).

Modeling of DCV p.L1503P (Type 2M)

Structural comparison of the hypothetical *in silico* model of type I collagen (3HQV) with the WT-VWF (→ **Fig. 1A**) reveals a difference in conformation with the model of collagen with the VWF mutant p.L1503P (→ **Fig. 1B**), with a RMSD of 22.61 Å.

When comparing the crystal structure of the WT-VWF and mutated models by domain, a RMSD of 5.84 Å is observed between VWF-A1 domains and 5.48 Å for VWF-A2 domains. When comparing the VWF-A3 domains in both models, the RMSD is greater, at 32.34 Å. When considering the collagen binding alone, the RMSD between the WT-VWF and the p.L1503P mutant is 24.30 Å. This mutation implies a change in the β 1-sheet between two aliphatic amino acids with hydrophobic side chains. This residue L1503 is embedded in the hydrophobic core of the VWF-A2 domain, close to the ADAMTS-13 cleavage site. Proline is a cyclic amino acid with the secondary amino group held in a rigid conformation, therefore reducing the structural flexibility of the protein at that point, as the substituted α -amino group influences the protein folding by forcing a bend in the chain. In the WT-VWF model, L1503 forms strong H-bonds with L1540 at a distance of 2.88 Å and with Y1542 at 2.96 Å, both on the β 2-sheet. In the P1503 mutant, the proline loses the H-bond with p.L1540, only keeping the Y1542 strong H-bond at a closer distance (1.93 Å).

The large overall deviation from the WT-VWF model, especially in the interaction between VWF-A3 and collagen, highlights a loss of structural stability (−1.80 kcal/mol) which could be interfering with the collagen binding. The ADAMTS-13 cleavage site is not affected, according to the presence of normal VWF multimers and normal values of VWFpp/Ag in patients. In addition, the high values of FVIII:-

C/Ag in 50% of patients suggested either reduced synthesis or intracellular retention of this DCV.

Modeling of DCV p.G1505R (Type 2A)

Structural comparison of the model of type I collagen with the WT-VWF model with the VWF mutant p.G1505R also reveals a difference in conformation with a RMSD of 15.08 Å. In this case, the conformational difference resides only in the VWF-A3 domain (RMSD: 15.41 Å) and with the collagen binding (RMSD: 55.56 Å), as the RMSD comparing VWF-A1 and VWF-A2 domains between the WT-VWF and the p.G1505R is 0.32 Å. This mutation occurs in the loop between the β 1-sheet and α 1-helix which, although not accessible, is close to the protein surface. This mutation changes the small, nonpolar aliphatic amino acid glycine to arginine, a larger amino acid with a positive side chain. Because the amino acid is embedded in the protein, this mutation requires structural changes with a decrease of VWF stability (−0.68 kcal/mol). The arginine forms the same strong H-bond that is present in the WT-VWF model with Y1542 (2.84 Å), which is in the loop between β 2- and β 3-sheets, but adds a new strong H-bond with E1504 (2.68 Å) in the β 1-sheet, which is not present in the WT-VWF. The inclusion of a positive larger residue plus the new strong H-bond in close proximity to the ADAMTS-13 cleavage site could induce structural rearrangements causing deviations from the WT-VWF model in the interaction between VWF-A3 and collagen sites, and also could explain the VWF hypersensitivity to proteolysis in plasma (2A-II phenotype), as seen by high values of VWFpp/Ag in patients.

Modeling of DCV p.Y1542D (Type 2A)

The p.Y1542D is slightly embedded in the hydrophobic core. This mutation of the β 2-sheet changes tyrosine, an amino acid with an aromatic residue, to aspartate, a negatively charged acidic amino acid, and resulted in a large decrease of VWF stability (−1.07 kcal/mol). Tyrosine forms strong H-bonds with L1503 (2.96 Å), G1505 (2.88 Å), and T1578 (2.80 Å), and another weak H-bond with T1578 (3.37 Å). Aspartate forms H-bonds with the loop between the β 1-sheet and α 1-helix at G1505 (2.84 Å) and L1503 (2.96 Å), losing the strong H-bond with α 3-helix at T1578, which could make the VWF-A2 domain more vulnerable to shear stress. The p.Y1542D was found in a 2-year-old girl with type 2A phenotype. Her relatives (parents and sister) were asymptomatic with normal laboratory tests; none of them were carriers of the daughter's variant. The haplotype analysis using four intragenic markers in the two generations of this family revealed that the p.Y1542D had arisen *de novo* in the patient (the second generation). The model of the p.Y1542D docked with collagen showed few differences (RMSD of 1.75 Å) with the WT-VWF model, also docked with type I collagen. The high values of FVIII:C/Ag in patients suggested either reduced synthesis or intracellular retention of this VWF mutant.

Modeling of DCV p.E1549K (Type 2M)

The p.E1549K is located in the β 3-sheet of the central hydrophobic core of the VWF-A2 domain. The RMSD between the

The VWF model with collagen using the WT-VWFA2 domain showed a RMSD of 24.44 Å with the model using VWFA2 mutant p.E1549K (► **Fig. 1C**). The VWF-A1 domains differ by a RMSD of 19.43 Å, VWF-A2 domains by 25.05 Å, VWF-A3 by 24.93 Å, and collagen 41.38 Å. This is the variant of glutamate with a negatively charged acidic group containing a second carboxyl group to the positively charged basic group amino acid lysine, with a second amino group on its aliphatic side chain. Glutamate forms two weak H-bonds with V1539 (2.74 Å), while the mutant with lysine forms no H-bond. The p.E1549K resulted in a decrease of VWF stability (−0.81 kcal/mol). The change in charge and size of the residue in the DCV and loss of H-bonds seem to induce a conformation change in the VWF-A3 domain affecting collagen binding and in the VWF-A1 domain affecting VWF-GP1b binding (or enhancing VWF-A1 stability thus reducing A1 unfolding under flow). In addition, the high values of VWFpp/Ag in 43.7% of the patients suggest a pathophysiological mechanism related to reduced survival of the VWF mutant. The findings of both normal VWFpp/Ag and FVIII:C/Ag in 56.3% of cases suggest that another unknown pathophysiological mechanism is probably involved.

Modeling of DCV p.R1564W (Type 2M)

In the VWF mutant p.R1564W there is also a change from arginine to tryptophan, but in this case the mutation is found in the α 2-helix embedded in the hydrophobic core of the VWF-A2 domain. This DCV changes the protein structure to expose the tryptophan residue. The comparison with the WT-VWF model shows RMSD differences greater than 20 Å in all domains and of 50.49 Å with collagen. The WT-VWF model shows that arginine forms weak H-bonds with D1560 (3.27 Å), I1568 (3.08 Å), and E1567 (2.91 Å), while tryptophan forms stronger H-bonds with the residues D1560 (2.05 Å), I1568 (1.96 Å), and E1567 (2.18 Å). The p.R1564W resulted in neutral VWF stability (−0.17 kcal/mol). The increased accessibility of the tryptophan residue and the loss of the positive charge of the arginine guanidino group together with the gain of H-bonds seem to induce steric hindrance causing substantial destabilizing effect on the VWF-A1 and VWF-A3 domains, affecting both VWF-GP1b and VWF-collagen binding. The high values of FVIII:C/Ag in patients suggested either reduced synthesis or intracellular retention of this VWF mutant.

Modeling of DCV p.R1597W (Type 2A)

The model for the VWF with the VWF-A2 mutant p.R1597W was also compared with the WT-VWF model, both docked with collagen. The R1597 is found embedded in the protein on the longest loop of the VWF-A2 domain, between α 3-helix and β 4-sheet. The R1597 stabilizes the loop through multiple H-bonds with the β 1-sheet at S1534 (2.91 Å) and D1498 (2.91 Å) and with the loop between α 3-helix and β 4-sheet at A1600 (3.02 Å). The p.R1597W changes arginine, an amino acid with a positive side chain, to tryptophan, an aromatic amino acid with a hydrophobic long side chain which is now exposed on the surface of the protein. This basic amino acid contains a guanidine group and the nitrogen of the indole

ring makes it polar. The RMSD is 0.37 Å, around 0.40 Å between VWF-A1, VWF-A2, and VWF-A3 domains and only 1.71 Å with type I collagen. The structural change in the mutant is not so evident, but although tryptophan still forms the same strong H-bond with D1498 (2.91 Å) and A1600 (3.02 Å), there is loss of the H-bond with the β 1-sheet at S1534. This change probably exposes the tryptophan, making it accessible to ADAMTS-13, thereby inducing increased VWF-A2 proteolysis in plasma with subsequent loss of HMWM. The p.R1597W resulted in neutral VWF stability (−0.41 kcal/mol). In addition, the high values of VWFpp/Ag in all the patients suggest a pathophysiological mechanism related to reduced VWF survival; a high FVIII:C/Ag in 31.2% of patients (reduced survival or intracellular retention of VWF mutant) suggests a combination of both pathophysiological mechanisms.

Modeling of DCV p.L1603P

The DCV p.L1603P change occurs between two aliphatic hydrophobic side-chain amino acids. Proline is smaller and the secondary amino group held in a rigid conformation reduces the structural flexibility of the protein at that point, probably interfering with the ADAMTS-13 proteolysis, given its close location to the ADAMTS-13 cleavage site, thus resulting in a type 2A phenotype.³⁹ According to Zhang and coworkers, this change could affect the van der Waals interaction with C1669-C1670, thus affecting the unfolding of the A2 domain.⁴⁰ L1603 forms a strong H-bond with N1498 (2.96 Å), and with A1500 (2.85 Å), while P1603 only keeps a strong H-bond with A1500 (2.85 Å). It was described that L1603, located within approximately 10 Å of the scissile bond Y1605-M1606, has an essential role in proteolysis for ADAMTS-13; its substitution to S, N, or K all reduced the cleavage efficiency, up to >400-fold.⁴¹ The p.L1603P resulted in a large decrease of VWF stability (−0.94 kcal/mol). However, this DCV was found in combination with two more genetic variants and in only one patient with normal VWFpp/Ag and a minimum rise of FVIII:C/Ag; therefore, another unknown pathophysiological mechanism is probably involved.

Modeling of DCV p.I1628T

The DCV p.I1628T is in the β 5-sheet also in the hydrophobic core of the VWF-A2 domain. This mutation changes the aliphatic nonpolar methyl-containing amino acid isoleucine to the hydroxyl-containing polar amino acid threonine, therefore adding a polar residue into the hydrophobic core resulting in a large decrease of VWF stability (−1.98 kcal/mol). An overall RMSD of 18.65 Å is observed when comparing the whole models for WT-VWF and mutated p.I1628T. When comparing the crystal structure of the WT-VWF and mutated model by domain, a RMSD of 14.25 Å is observed between VWF-A1 domains, 19.72 Å for VWF-A2 domains, and 10.71 Å for VWF-A3 domains. When considering the collagen binding alone, the RMSD between the WT-VWF and the p.I1628T mutant is 50.23 Å. Isoleucine forms H-bonds with M1606 (2.76 Å) and T1608 (3.09 Å) at the ADAMTS-13 cleavage site in the middle of the β 4 strand, while threonine forms stronger

H-bonds with these residues: M1606 (1.91 Å) and T1608 (2.19 Å), perhaps making it harder for ADAMTS-13 to access the cleavage site. However, both, the high VWFpp/Ag observed in 50% of patients and high FVIII:C/Ag in 33.3% of patients, would suggest a combination of both pathophysiological mechanisms. In addition, the large overall deviation from the WT-VWF model, especially in the interaction between the VWF-A3 domain and collagen, highlights a loss of structural stability which could be interfering with the collagen binding.

Modeling of DCV p.G1631D (Type 2A)

This DCV p.G1631D occurs in the loop between β 5-sheet and α 4-helix, changing the nonpolar aliphatic amino acid glycine to aspartate, a negatively charged acidic amino acid, resulting in a large decrease of VWF stability (-0.90 kcal/mol). The overall RMSD between the models is of 13.85 Å. The VWF-A1 domain's difference is 6.55 Å, VWF-A2 domain 6.09 Å, VWF-A3 domain 17.82 Å, and collagen 36.38 Å. Glycine shows two strong H-bonds with I1651 (2.97 and 2.78 Å) and two weak bonds with A1634 (3.39 and 3.25 Å). The aspartate mutant only has one bond with I1651 but this is stronger (2.08 Å), one stronger bond with A1634 is maintained (1.92 Å) plus three new H-bonds with N1633 (1.89, 2.12, and 2.19 Å) that did not exist in the WT-VWF model. According to these results, the change in conformation and the RMSD deviation from the WT-VWF model, especially in the interaction between the VWF-A3 domain and collagen, highlight a loss of structural stability which could be interfering with the type I collagen binding, with a lower effect on VWF-GP1b binding. The high VWFpp/Ag and normal FVIII:C/Ag suggest a pathophysiological mechanism related to reduced VWF survival, not related to ADAMTS-13 cleavage, given the previous description that residues G1624 to R1641 are not essential for ADAMTS-13 cleavage.⁴²

Modeling of DCV p.F1654L (Type 2A)

The p.F1654L is located in the α 6-helix, very close to the protein surface. The amino acid phenylalanine, with a hydrophobic aromatic side chain, is mutated to leucine, a nonpolar amino acid with a nonaromatic smaller hydrophobic side chain. This DCV causes a great structural change resulting in a large decrease of VWF stability (-0.94 kcal/mol), which could explain the lack of HMWM and IMWM observed in the patient. The comparison of the WT-VWF model and the mutant showed a RMSD of 24.00 Å, with all the VWF domains differing in around 20 Å and collagen with a RMSD of 50.52 Å. This DCV did not show changes in the amount of H-bonds, as neither the WT-VWF nor the mutant presented any bonds in this residue. In addition, as observed before, the change in conformation and the RMSD deviation from the WT-VWF model, especially in the interaction between the VWF-A3 domain and collagen, highlights a loss of structural stability which could be interfering with the collagen binding. Both VWFpp/Ag and FVIII:C/Ag were normal; therefore, another unknown pathophysiological mechanism seems to be involved.

Modeling of DCV p.R1374C Located in the VWF-A1 Domain, as Control

The model of the most common mutation in the VWF-A1 domain (p.R1374C) used as a control docked with collagen showed few differences (RMSD of 0.26 Å) with the WT-VWF model, also docked with type I collagen.

Discussion

In the current study, we describe the differences in clinical and laboratory profiles for patients and families with type 2A or 2M VWD according to the domain affected by DCVs and the proposed pathophysiological mechanisms involved.

As has previously been reported,⁴³ we did not find a relationship between FVIII:C, VWF:RCo, and VWFpp/Ag levels in regard to major bleeding occurrence. However, as reported by Castaman et al,⁴⁴ our type 2A patients also showed a higher frequency of major bleeding episodes/patient than type 2M patients, probably due to the absence of HMWM and IMWM of VWF in the 2A patients, in addition to VWF functional defects.

According to previous reports,^{12,45,46} our type 2A and 2M patients carrying the same DCV showed variable bleeding scores not only in the same family but also among families. Accordingly, it seems reasonable to speculate on the involvement of modifier genes^{13,47} on the clinical phenotype of these patients.

It is well known that VWF:RCo evaluates VWF-A1 domain-platelet binding, whereas VWF:CB reflects a different functional property of VWF than VWF:RCo,⁴⁸ namely, VWF-collagen binding. Both assays are sensitive to the absence of HMWM.⁴⁹ Accordingly, reduced C1B/Ag was shown in all our type 2A patients, being more decreased in those with DCV in the VWF-A2 domain.

In type 2M VWD patients, C1B was normal when DCVs were located in the VWF-A1 domain, whereas it was reduced when DCVs were located in the VWF-A2 domain. One probable speculative explanation for the higher frequency of major bleeding in these patients compared with those with DCV in the VWF-A1 domain could be a summative effect of abnormal C1B/Ag in these patients, on top of the reduced GPIb binding.

Our data regarding the differences found in VWF:C1B according to the location of the residue causing the DCVs especially in 2M VWD seem to reinforce the relevance of the VWF multimer analysis in the adequate VWD diagnosis, despite their limitations.

It has been described that the presence of DCV in certain domains could alter the functionality of their neighboring domain and influences the profile of associated bleeding.⁵⁰⁻⁵⁴ Influences of the VWF-A2 and VWF-D4 domains on the VWF-A3 domain-collagen binding have also been suggested.⁵⁵

The simulations using homology models (as there is no crystal structure of the whole VWF) show that DCVs distant from the collagen-binding site also affect structure and function of the VWF protein. However, there are limitations in the *in silico* modeling analysis, given that errors in the

model might cause conformational changes leading to misinterpretation of interactions. In some cases, the DCVs can affect synthesis, secretion, assembly, or folding of the proteins which are not contemplated in these simulations. The models used in this work include the three domains for VWF before the VWF-A2 domain is unfolded to react with ADAMTS-13, a protein which will join at the proteolytic site upon shear and after VWF has attached to the collagen fibers. Structural changes associated to this event are not taken into consideration. There is also a possibility that DCVs in the VWF-A2 domain could increase or decrease the stability of already an unstable domain, rendering it more or less resistant to proteolysis by ADAMTS-13 such as p.G1505R, p.R1597W, and p.G1631D. According to Sutherland et al, a single loop displacement near the proteolysis site caused by a mutation in amino acid R1597 could affect the interactions between VWF and the ADAMTS-13, resulting in enhanced access to the Y1605-M1606 cleavage site.⁵⁶ Moreover, the *in silico* modeling analysis of DCV located in the VWF-A2 domain also shows that the changes in the tertiary structure of this domain by DCVs would affect the VWF-A3 domain–type I collagen binding. This finding should be considered as one of the possible reasons for the low collagen binding in type 2M patients with DCV in the VWF-A2 domain.

Pathophysiological Mechanisms

The pathophysiological mechanisms involved in the type 2 VWD phenotype are variable; these have been described as enhanced clearance in 59 and 48% of types 2A and 2M patients respectively, reduced synthesis in 3% of type 2A, and a combination of both abnormal mechanisms in 32% of type 2A and 44% of type 2M.¹⁸ Neither increased VWF clearance nor reduced syntheses were observed in 6% of type 2A patients.¹⁸ In our type 2A patients, we found that the only p.C1272F located in the VWF-A1 domain showed only increased clearance, whereas p.G1505R, p.R1597W, and p.I1628T in the VWF-A2 domain resulted in a combination of both increased clearance and abnormal synthesis, though with prevalence of enhanced VWF clearance. According to these results, we propose here the p.Y1542D as a 2A-I group DCV, and the p.C1272F, p.G1505R, and p.R1597W as 2A-II group DCVs. The 2A-I group DCVs have been described as altered proteins due to a defective biosynthesis or intracellular retention,⁵⁷ and the 2A-II group DCVs as those with an increased susceptibility to ADAMTS-13 proteolysis.⁵⁸ However, some DCVs do not fit clearly into either group.⁵⁹ DCVs belonging to the 2A-I group result in a more severe phenotype than the 2A-II group; patients carrying the latter DCVs respond better to treatment with DDAVP.⁶⁰ In line with these observations, and according to the clinical symptoms of our patients, we had previously speculated that p.C1272F substitution would also be consistent with the 2A-I group DCVs²⁹ in spite of having high VWFpp/Ag, which would be consistent with the 2A-II group DCVs. Similarly, p.G1505R, previously described as a 2A-I group DCV,⁶¹ in our patient, according to the high VWFpp/Ag, would be consistent with the 2A-II group DCV.

In our type 2M patients, DCVs in the VWF-A1 domain were responsible for not only a reduced VWF synthesis but also an enhanced VWF clearance. The presence of both abnormal pathophysiological mechanisms mainly in this domain would be responsible for the lower levels of VWF:Ag observed. When DCVs were located in the VWF-A2 domain, these findings were observed in a minor extent. Given that 47.6% of the cases showed both normal mechanisms, DCVs in the VWF-A2 domain would affect VWF–platelet binding, without altering the normal synthesis/secretion and clearance of mutant VWF. These findings can provide insight into the pathophysiological mechanism of DCV within VWF-A1 and VWF-A2 domains in type 2M VWD. Other nonidentified mechanisms may play a role mainly in type 2M VWD where both normal FVIII:C/Ag and VWFpp/Ag were found.

Phenotype–Genotype Discordances

It was reported that the combination of several genetic variants in the VWF gene could modify the phenotype.^{12,62,63} Overall, a strong phenotype–genotype correlation was observed in our cohort of patients, except in one patient whose genotype did not correlate with her type 2A VWD phenotype, probably due to the combined effect of the presence of p.P1266Q described as type 2M VWD and type 2B VWD, p.L1603P, as type 1 VWD and type 2A VWD phenotype, and the novel variant p.R1379H, which showed a nondefined phenotype.

On the other hand, p.G1324S has been described to be associated to the type 2M VWD phenotype (<http://www.ragtimedesign.com/vwf/mutation>) with a minimal mucocutaneous bleeding history⁶⁴; in our VWD cohort, the patient with this DCV had severe bleeding with a bleeding score of 20. Another discrepancy was observed with p.I1628T; those six patients with absence of HMWM of VWF and high VWFpp/Ag and therefore diagnosed as type 2A VWD group II showed higher both major bleeding and bleeding score than those with the normal multimeric pattern (type 2M VWD). This DCV was described as a type 2A VWD phenotype.^{56,60} Apart from the different multimeric patterns between these patients, there was no further explanation for our discrepancy.

Our current study has some limitations. To better define pathophysiological mechanisms involved in DCVs responsible for type 2A and 2M VWD, the number of patients could be increased and additional expression studies are also needed to complete this point. In addition, use of whole genome or exome might be very useful to detect other genetic determinants which influence the phenotype.

Conclusion

Our results show that type 2A VWD has a more severe clinical profile and more an abnormal laboratory phenotype than type 2M VWD, and the associated pathophysiological mechanisms are related to a reduced VWF half-life, regardless of the location of the DCVs. However, within type 2A VWD, when the DCVs were located in the VWF-A1 domain, these findings were more severe.

In type 2M VWD, DCVs located in the VWF-A1 domain appeared to be responsible for both reduced synthesis/retention and reduced VWF half-life, whereas those located in the VWF-A2 domain were responsible mainly for a reduced VWF half-life, and impaired VWF:C1B via the VWF-A3 domain, suggesting that the conformational changes of the VWF-A2 domain by DCVs would affect the neighboring VWF-A3 domain thus altering the VWF-C1B binding.

The findings of both normal FVIII:C/Ag and VWFpp/Ag mainly in type 2M VWD would suggest the presence of some nonidentified pathophysiological mechanisms responsible for the phenotype that would be related to neither synthesis/retention nor survival of VWF.

We believe that this new information can help to achieve a correct classification of patients, through better knowledge of the pathophysiological mechanisms involved in type 2A and 2M VWD and therefore on the VWF molecule.

Funding

This work was supported by CONICET, Fundación Rene Barón, and Academia Nacional de Medicina (Buenos Aires), Argentina.

Conflict of Interest

None declared.

Acknowledgments

We are grateful to Mrs. Maria Marta Casinelli for her excellent technical assistance.

References

- Sadler JE, Budde U, Eikenboom JC, et al; Working Party on von Willebrand Disease Classification. Update on the pathophysiology and classification of von Willebrand disease: a report of the Subcommittee on von Willebrand Factor. *J Thromb Haemost* 2006;4(10):2103–2114
- Favaloro EJ, Bonar RA, Mohammed S, et al. Type 2M von Willebrand disease - more often misidentified than correctly identified. *Haemophilia* 2016;22(03):e145–e155
- Woods AI, Kempfer AC, Paiva J, Blanco AN, Sánchez-Luceros A, Lazzari MA. Diagnosis of von Willebrand disease in Argentina: a single institution experience. *Ann Blood* 2017;2:22
- Swami A, Kaur V. von Willebrand disease: a concise review and update for the practicing physician. *Clin Appl Thromb Hemost* 2017;23(08):900–910
- Favaloro EJ, Oliver S, Mohammed S, Vong R. Comparative assessment of von Willebrand factor multimers vs activity for von Willebrand disease using modern contemporary methodologies. *Haemophilia* 2020;26(03):503–512
- Laffan MA, Lester W, O'Donnell JS, et al. The diagnosis and management of von Willebrand disease: a United Kingdom Haemophilia Centre Doctors Organization guideline approved by the British Committee for Standards in Haematology. *Br J Haematol* 2014;167(04):453–465
- Lillicrap D. Von Willebrand disease - phenotype versus genotype: deficiency versus disease. *Thromb Res* 2007;120(Suppl 1):S11–S16
- Berntorp E, Ågren A, Aledort L, et al. Fifth Åland Island conference on von Willebrand disease. *Haemophilia* 2018;24(Suppl 4):5–19
- Baroncini L, Goodeve A, Peyvandi F. Molecular diagnosis of von Willebrand disease. *Haemophilia* 2017;23(02):188–197
- Zolkova J, Sokol J, Simurda T, et al. Genetic background of von Willebrand disease: history, current state, and future perspectives. *Semin Thromb Hemost* 2020;46(04):484–500
- Favaloro EJ, Pasalic L, Curnow J. Type 2M and type 2A von Willebrand disease: similar but different. *Semin Thromb Hemost* 2016;42(05):483–497
- Doruelo AL, Haberichter SL, Christopherson PA, et al. Clinical and laboratory phenotype variability in type 2M von Willebrand disease. *J Thromb Haemost* 2017;15(08):1559–1566
- Fidalgo T, Oliveira A, Silva Pinto C, et al. VWF collagen (types III and VI)-binding defects in a cohort of type 2M VWD patients - a strategy for improvement of a challenging diagnosis. *Haemophilia* 2017;23(02):e143–e147
- Tischer A, Campbell JC, Machha VR, et al. Mutational constraints on local unfolding inhibit the rheological adaptation of von Willebrand factor. *J Biol Chem* 2016;291(08):3848–3859
- Keeling D, Beavis J, Marr R, Sukhu K, Bignell P. A family with type 2M VWD with normal VWF:RCO but reduced VWF:CB and a M1761K mutation in the A3 domain. *Haemophilia* 2012;18(01):e33
- Flood VH, Lederman CA, Wren JS, et al. Absent collagen binding in a VWF A3 domain mutant: utility of the VWF:CB in diagnosis of VWD. *J Thromb Haemost* 2010;8(06):1431–1433
- Eikenboom J, Federici AB, Dirven RJ, et al; MCMDM-1VWD Study Group. VWF propeptide and ratios between VWF, VWF propeptide, and FVIII in the characterization of type 1 von Willebrand disease. *Blood* 2013;121(12):2336–2339
- Sanders YV, Groeneveld D, Meijer K, et al; WiN study group. von Willebrand factor propeptide and the phenotypic classification of von Willebrand disease. *Blood* 2015;125(19):3006–3013
- Eikenboom JC, Castaman G, Kamphuisen PW, Rosendaal FR, Bertina RM. The factor VIII/von Willebrand factor ratio discriminates between reduced synthesis and increased clearance of von Willebrand factor. *Thromb Haemost* 2002;87(02):252–257
- Rodeghiero F. Bleeding score and bleeding questionnaire for the diagnosis of type 1 von Willebrand disease. Accessed 2021 at: https://cdn.ymaws.com/www.isth.org/resource/resmgr/ssc/bleeding_type1_vwd.pdf
- Bowman M, Riddel J, Rand ML, Tosoetto A, Silva M, James PD. Evaluation of the diagnostic utility for von Willebrand disease of a pediatric bleeding questionnaire. *J Thromb Haemost* 2009;7(08):1418–1421
- Janssen CA, Scholten PC, Heintz AP. A simple visual assessment technique to discriminate between menorrhagia and normal menstrual blood loss. *Obstet Gynecol* 1995;85(06):977–982
- Schulman S, Kearon C Subcommittee on Control of Anticoagulation of the Scientific and Standardization Committee of the International Society on Thrombosis and Haemostasis. Definition of major bleeding in clinical investigations of antihemostatic medicinal products in non-surgical patients. *J Thromb Haemost* 2005;3(04):692–694
- Duncan E, Rodgers S. One-stage factor VIII assays. *Methods Mol Biol* 2017;1646:247–263
- Favaloro EJ, Mohammed S, Patzke J. Laboratory testing for von Willebrand factor antigen (VWF:Ag). *Methods Mol Biol* 2017;1646:403–416
- Mohammed S, Favaloro EJ. Laboratory testing for von Willebrand factor ristocetin cofactor (VWF:RCO). *Methods Mol Biol* 2017;1646:435–451
- Stufano F, Boscarino M, Bucciarelli P, et al. Evaluation of the utility of von Willebrand factor propeptide in the differential diagnosis of von Willebrand disease and acquired von Willebrand syndrome. *Semin Thromb Hemost* 2019;45(01):36–42
- Farias C, Kempfer AC, Blanco A, Woods A, Lazzari MA. Visualization of the multimeric structure of von Willebrand factor by immunoenzymatic stain using avidin-peroxidase complex instead of avidin-biotin peroxidase complex. *Thromb Res* 1989;53(05):513–518

- 29 Woods AI, Sanchez-Luceros A, Kempfer AC, et al. C1272F: a novel type 2A von Willebrand's disease mutation in A1 domain; its clinical significance. *Haemophilia* 2012;18(01):112–116
- 30 Guex N, Peitsch MC. SWISS-MODEL and the Swiss-PdbViewer: an environment for comparative protein modeling. *Electrophoresis* 1997;18(15):2714–2723
- 31 Kozakov D, Hall DR, Xia B, et al. The ClusPro web server for protein-protein docking. *Nat Protoc* 2017;12(02):255–278
- 32 Schneidman-Duhovny D, Inbar Y, Nussinov R, Wolfson HJ. Patch-Dock and SymmDock: servers for rigid and symmetric docking. *Nucleic Acids Res* 2005;33(Web Server issue):W363–7
- 33 Laskowski RA, Jabłońska J, Pravda L, Vařeková RS, Thornton JM. PDBsum: structural summaries of PDB entries. *Protein Sci* 2018;27(01):129–134
- 34 Pettersen EF, Goddard TD, Huang CC, et al. UCSF Chimera—a visualization system for exploratory research and analysis. *J Comput Chem* 2004;25(13):1605–1612
- 35 Agresti A, Coull BA. Approximate is better than 'exact' for interval estimation of binomial proportions. *Am Stat* 1998;52:119–126
- 36 Ahmad F, Jan R, Kannan M, et al. Characterisation of mutations and molecular studies of type 2 von Willebrand disease. *Thromb Haemost* 2013;109(01):39–46
- 37 Ahmad F, Kannan M, Obser T, et al. Characterization of VWF gene conversions causing von Willebrand disease. *Br J Haematol* 2019;184(05):817–825
- 38 Federici AB, Bucciarelli P, Castaman G, et al. Management of inherited von Willebrand disease in Italy: results from the retrospective study on 1234 patients. *Semin Thromb Hemost* 2011;37(05):511–521
- 39 Berber E, Pehlevan F, Akin M, Capan OY, Kavakli K, Çağlayan SH. A common VWF exon 28 haplotype in the Turkish population. *Clin Appl Thromb Hemost* 2013;19(05):550–556
- 40 Zhang Q, Zhou YF, Zhang CZ, Zhang X, Lu C, Springer TA. Structural specializations of A2, a force-sensing domain in the ultralarge vascular protein von Willebrand factor. *Proc Natl Acad Sci U S A* 2009;106(23):9226–9231
- 41 Xiang Y, de Groot R, Crawley JT, Lane DA. Mechanism of von Willebrand factor scissile bond cleavage by a disintegrin and metalloproteinase with a thrombospondin type 1 motif, member 13 (ADAMTS13). *Proc Natl Acad Sci U S A* 2011;108(28):11602–11607
- 42 Gao W, Anderson PJ, Sadler JE. Extensive contacts between ADAMTS13 exosites and von Willebrand factor domain A2 contribute to substrate specificity. *Blood* 2008;112(05):1713–1719
- 43 Larsen DM, Haberichter SL, Gill JC, Shapiro AD, Flood VH. Variability in platelet- and collagen-binding defects in type 2M von Willebrand disease. *Haemophilia* 2013;19(04):590–594
- 44 Castaman G, Federici AB, Tosoletto A, et al. Different bleeding risk in type 2A and 2M von Willebrand disease: a 2-year prospective study in 107 patients. *J Thromb Haemost* 2012;10(04):632–638
- 45 James PD, Notley C, Hegadorn C, et al; Association of Hemophilia Clinic Directors of Canada. Challenges in defining type 2M von Willebrand disease: results from a Canadian cohort study. *J Thromb Haemost* 2007;5(09):1914–1922
- 46 Hilbert L, Fressinaud E, Ribba AS, Meyer D, Mazurier CINSERM network on molecular abnormalities in von Willebrand disease. Identification of a new type 2M von Willebrand disease mutation also at position 1324 of von Willebrand factor. *Thromb Haemost* 2002;87(04):635–640
- 47 Sanders YV, van der Bom JG, Isaacs A, et al; WiN Study Group. CLEC4M and STXB5 gene variations contribute to von Willebrand factor level variation in von Willebrand disease. *J Thromb Haemost* 2015;13(06):956–966
- 48 Favaloro EJ. An update on the von Willebrand factor collagen binding assay: 21 years of age and beyond adolescence but not yet a mature adult. *Semin Thromb Hemost* 2007;33(08):727–744
- 49 Favaloro EJ, Bonar R, Chapman K, Meiring M, Funk Adcock D. Differential sensitivity of von Willebrand factor (VWF) 'activity' assays to large and small VWF molecular weight forms: a cross-laboratory study comparing ristocetin cofactor, collagen-binding and mAb-based assays. *J Thromb Haemost* 2012;10(06):1043–1054
- 50 Auton M, Sowa KE, Smith SM, Sedlák E, Vijayan KV, Cruz MA. Destabilization of the A1 domain in von Willebrand factor dissociates the A1A2A3 tri-domain and provokes spontaneous binding to glycoprotein Ibalph and platelet activation under shear stress. *J Biol Chem* 2010;285(30):22831–22839
- 51 Nishio K, Anderson PJ, Zheng XL, Sadler JE. Binding of platelet glycoprotein Ibalph to von Willebrand factor domain A1 stimulates the cleavage of the adjacent domain A2 by ADAMTS13. *Proc Natl Acad Sci U S A* 2004;101(29):10578–10583
- 52 Lankhof H, Damas C, Schiphorst ME, et al. von Willebrand factor without the A2 domain is resistant to proteolysis. *Thromb Haemost* 1997;77(05):1008–1013
- 53 Martin C, Morales LD, Cruz MA. Purified A2 domain of von Willebrand factor binds to the active conformation of von Willebrand factor and blocks the interaction with platelet glycoprotein Ibalph. *J Thromb Haemost* 2007;5(07):1363–1370
- 54 Butera D, Passam F, Ju L, et al. Autoregulation of von Willebrand factor function by a disulfide bond switch. *Sci Adv* 2018;4(02):eaq1477
- 55 van der Plas RM, Gomes L, Marquart JA, et al. Binding of von Willebrand factor to collagen type III: role of specific amino acids in the collagen binding domain of vWF and effects of neighboring domains. *Thromb Haemost* 2000;84(06):1005–1011
- 56 Sutherland JJ, O'Brien LA, Lillcrap D, Weaver DF. Molecular modeling of the von Willebrand factor A2 domain and the effects of associated type 2A von Willebrand disease mutations. *J Mol Model* 2004;10(04):259–270
- 57 Kashiwagi T, Matsushita T, Ito Y, et al. L1503R is a member of group I mutation and has dominant-negative effect on secretion of full-length VWF multimers: an analysis of two patients with type 2A von Willebrand disease. *Haemophilia* 2008;14(03):556–563
- 58 Hassenpflug WA, Budde U, Obser T, et al. Impact of mutations in the von Willebrand factor A2 domain on ADAMTS13-dependent proteolysis. *Blood* 2006;107(06):2339–2345
- 59 Jacobi PM, Gill JC, Flood VH, Jakab DA, Friedman KD, Haberichter SL. Intersection of mechanisms of type 2AVWD through defects in VWF multimerization, secretion, ADAMTS-13 susceptibility, and regulated storage. *Blood* 2012;119(19):4543–4553
- 60 Michiels JJ, van Vliet HH. Dominant von Willebrand disease type 2A groups I and II due to missense mutations in the A2 domain of the von Willebrand factor gene: diagnosis and management. *Acta Haematol* 2009;121(2–3):154–166
- 61 Lynch CJ, Cawte AD, Millar CM, Rueda D, Lane DA. A common mechanism by which type 2A von Willebrand disease mutations enhance ADAMTS13 proteolysis revealed with a von Willebrand factor A2 domain FRET construct. *PLoS One* 2017;12(11):e0188405
- 62 Pagliari MT, Baronciani L, Stufano F, et al. von Willebrand disease type 1 mutation p.Arg1379Cys and the variant p.Ala1377Val synergistically determine a 2M phenotype in four Italian patients. *Haemophilia* 2016;22(06):e502–e511
- 63 Woods AI, Paiva J, Kempfer AC, et al. Combined effects of two mutations in von Willebrand disease 2M phenotype. *Res Pract Thromb Haemost* 2017;2(01):162–167
- 64 Bowman M, Rimmer E, Houston DS, Israels SJ, James P. Discordant von Willebrand factor (VWF) activity in patients with VWF p. Gly1324Ser confirmed in vitro. *Haemophilia* 2018;24(02):e57–e59